Cement and Concrete Research 42 (2012) 397–403

Contents lists available at SciVerse ScienceDirect

Cement and Concrete Research

journal homepage: http://ees.elsevier.com/CEMCON/default.asp

Experimental determination of bulk modulus of 14 Å tobermorite using high pressure synchrotron X-ray diffraction

Jae Eun Oh [a,b], Simon M. Clark [c,d], Hans-Rudolf Wenk [c], Paulo J.M. Monteiro [a,*]

[a] Department of Civil and Environmental Engineering, University of California, Berkeley, 94720, CA USA
[b] School of Urban and Environmental Engineering, Ulsan National Institute of Science and Technology, Ulsan Metropolitan City, 689-798, South Korea
[c] Department of Earth and Planetary Sciences, Maquarie University, Sydney, NSW 2109, Australia
[d] Advanced Light Source, Lawrence Berkeley National Laboratory, Berkeley, 20015, CA, USA

ARTICLE INFO

Article history:
Received 16 August 2011
Accepted 9 November 2011

Keywords:
C–S–H (B)
X-ray diffraction (B)
Elastic moduli (C)
Mechanical properties (C)
14 Å tobermorite

ABSTRACT

Using a diamond anvil cell, 14 Å tobermorite, a structural analogue of calcium silicate hydrates (C–S–H), was examined by high-pressure synchrotron X-ray diffraction up to 4.8 GPa under hydrostatic conditions. The bulk modulus of 14 Å tobermorite was calculated, $K_o = 47$ GPa. Comparison of the current results with previous high pressure studies on C–S–H(I) indicates that: (1) the compression behavior of the lattice parameters ***a*** and ***b*** of 14 Å tobermorite and C–S–H(I) are very similar, implying that both materials may have very similar Ca–O layers, and also implying that an introduction of structural defects into the Ca–O layers may not substantially change in-plane incompressibility of the ***ab*** plane of 14 Å tobermorite; and (2) the bulk modulus values of 14 Å tobermorite and C–S–H(I) are dominated by the incompressibility of the lattice parameter ***c***, which is directly related to the interlayer spacing composed of dreierketten silicate chains, interlayer Ca, and water molecules.

1. Introduction

The world consumes over 17 billion tons of portland cement concrete per year, making it the second largest volume material used in the world after water. The most important hydration product of portland cement is calcium silicate hydrate (C–S–H), which makes up over half of the volume of hydrated cement paste and is the primary source of strength. Understanding the properties of C–S–H is important to better control the nanoporosity of the hydrated paste – leading to more durable reinforced structures – and to potentially increase incorporating industrial waste products, which can change the type of C–S–H produced. A major limitation to maximizing the potential of this material is the limited understanding of its atomic structure, primarily due to the experimental difficulties in dealing with a poorly crystalline material. Each leap forward in understanding the nature of C–S–H has resulted in the application of novel experimental techniques [1–3] or theoretical advances [4].

Up to now, the crystal structure and mechanical behavior of C–S–H at the nanoscale was not well understood because C–S–H is nearly amorphous to X-rays. Structural models for C–S–H have been proposed to account for experimentally observed properties of C–S–H, and those models are well summarized [4,5]. Taylor [6] first proposed one of the still relevant structural models of C–S–H, whereby C–S–H is described as a disordered layered structure consisting of a mixture of two distinct phases: 14 Å tobermorite (plombierite) and jennite. In this model, two different components are sandwiched together with small additional fragments of Ca–O layers and separated from each other on a nanometer length scale. The compositional variations of Ca/Si as well as structural disorder can be explained in terms of the omission of many silicate tetrahedra from dreierketten silicate chains [7]. Consequently, studies on the structural mineral analogues, 14 Å tobermorite (plombierite) and jennite, together with synthetic analogues such as calcium silicate hydrates I [C–S–H (I)] has played critical roles in understanding the real crystal structure of C–S–H [5]. The 14 Å tobermorite possesses a layered structure, with layers consisting mainly of sheets of CaO_7 polyhedra (called, Ca–O layer) parallel to (001) (see Fig. 1), and single chains of silicate tetrahedra (Si–O chain) flank the Ca–O layers and run along the [010] direction with a periodicity of three tetrahedra (called, 'dreierketten chain'). The structure of C–S–H(I) resembles 14 Å tobermorite, but it is more structurally disordered and closer to C–S–H.

The bulk modulus is one of the fundamental mechanical properties of structural materials, and a number of theoretical simulation studies [8–12] have investigated the bulk modulus of 14 Å tobermorite, based on a well-defined structure [13]. Although these atomistic simulations have been at the forefront in attempts to understand 14 Å tobermorite and C–S–H, there have been few experimental determinations of the bulk modulus of these materials, a parameter necessary for validating the theoretical models.

* Corresponding author. Tel.: +1 5106438251; fax: +1 5106435264.
E-mail address: monteiro@berkeley.edu (P.J.M. Monteiro).

0008-8846/$ – see front matter © 2011 Elsevier Ltd. All rights reserved.
doi:10.1016/j.cemconres.2011.11.004

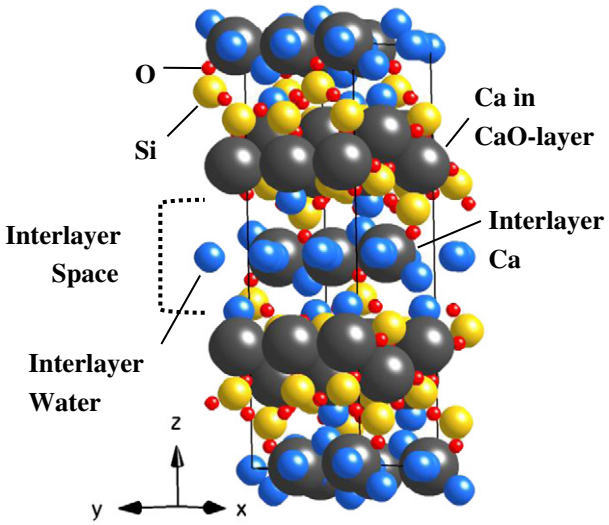

Fig. 1. Crystal structure of 14 Å tobermorite, refined by Bonaccorsi et al. [13].

Reported herein is the first experimentally determined bulk modulus of 14 Å tobermorite, which was accomplished by measuring the unit cell volume change with pressure increases up to 4.8 GPa. This result allows us to evaluate different theoretical approaches, provides key experimental observations that should be the baseline for future simulations, and suggests an appropriate strategy for future simulation studies.

2. Experimental program

The 14 Å tobermorite sample was obtained from Los Angeles County Museum of Natural History, which is the same specimen from Crestmore, California, studied by Bonaccorsi et al. [13]. The high-pressure X-ray diffraction experiment was carried out at beamline 12.2.2 of the Advanced Light Source of Lawrence Berkeley National Laboratory [14]. For this experiment, a synchrotron monochromatic X-ray beam with $\lambda = 0.6199$ Å was used; LaB_6 powder was used to calibrate the working distance between the sample and detector, as well as a detector for orientation. Diffraction patterns were recorded with a MAR345 image plate (3,450 × 3,450 pixels) with an exposure time of 300 s at room temperature, and analyzed with the FIT2D [15], XFIT [16] , CELREF [17] and MAUD [18] software programs.

The 14 Å tobermorite sample was finely ground and mixed with a pressure transmitting liquid medium (4:1 methanol/ethanol solution) to generate hydrostatic pressure [19], put into a small sample chamber of a steel gasket in the diamond anvil cell (DAC), and analyzed in axial geometry (see Fig. 2). Because this technique relies on a very small cylindrical sample chamber (180-μm diameter with 63-μm thickness), the utilized sample volume was also very small ($= \sim 1.6 \times 10^{-12}$ m^3). The pressure inside the sample chamber was determined using the corundum [Al_2O_3 doped with Cr^{3+} (0.05%)] fluorescence calibration method [20].

3. Results

X-ray diffraction patterns were collected at several steps as the pressure was increased up to 4.8 GPa. Fig. 3 shows two typical diffraction patterns, and Fig. 4 shows the whole set of one-dimensional integrated X-ray powder diffraction patterns as a function of pressure. Note that there is no distinct merging or separation of any diffracted peaks, implying that the high-pressure application did not change the symmetry of 14 Å tobermorite.

Measuring the bulk modulus of a material using the DAC is straightforward. As the hydrostatic pressure applied to a material increases, the unit cell of the material experiences changes in its lattice parameters. By analyzing the X-ray diffraction patterns collected under pressure, the lattice parameters at a certain pressure can be determined based on diffraction peak positions; from lattice parameters the unit-cell volume can be calculated.

To increase confidence in the results, the unit cell lattice parameters and the unit cell volumes are calculated in two different ways for the same diffraction spectra: First, lattice parameters were refined using the Rietveld method implemented in the software MAUD [18]. The Rietveld method uses the full spectrum and refines a model function based on instrumental parameters and the Bonaccorsi et al.'s crystal structure model (monoclinic system) [13]. During the Rietveld refinement, all atom positions (i.e., fractional coordinates of atoms in a unit cell) were fixed to the coordinates of the monoclinic 14 Å tobermorite structure at ambient conditions [13]. This is because the X-ray diffraction data were insufficient to perform a structural refinement, even considering the caveat that minor structural changes may occur with pressure. Fig. 5 shows the reasonable fit between the diffraction profile and the calculated fit.

Next, the unit cell parameters were refined using the software CELREF [17], which is based on peak positions of individual diffraction peaks and simple crystallographic information (i.e., space group and lattice parameters; no profile information is used). The CELREF produced high computational unreliability ($=\sigma$) for the parameters because the simulated peak positions from the CELREF did not match well with the experimentally identified peak positions from XFIT [16], and thus for the unit cell parameter refinement with CELREF, the Bonaccorsi et al.'s model could not be used. Note that the 14 Å tobermorite is not a well crystalline mineral and thus the experimental peak positioning

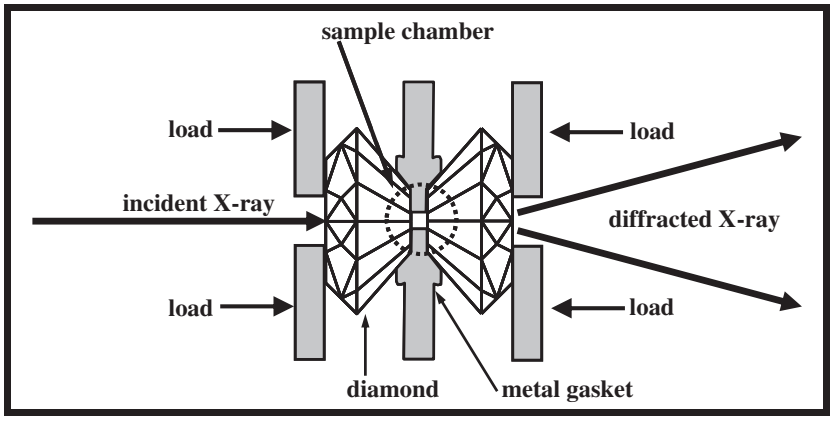

Fig. 2. Schematic view of high pressure X-ray diffraction using a diamond anvil cell.

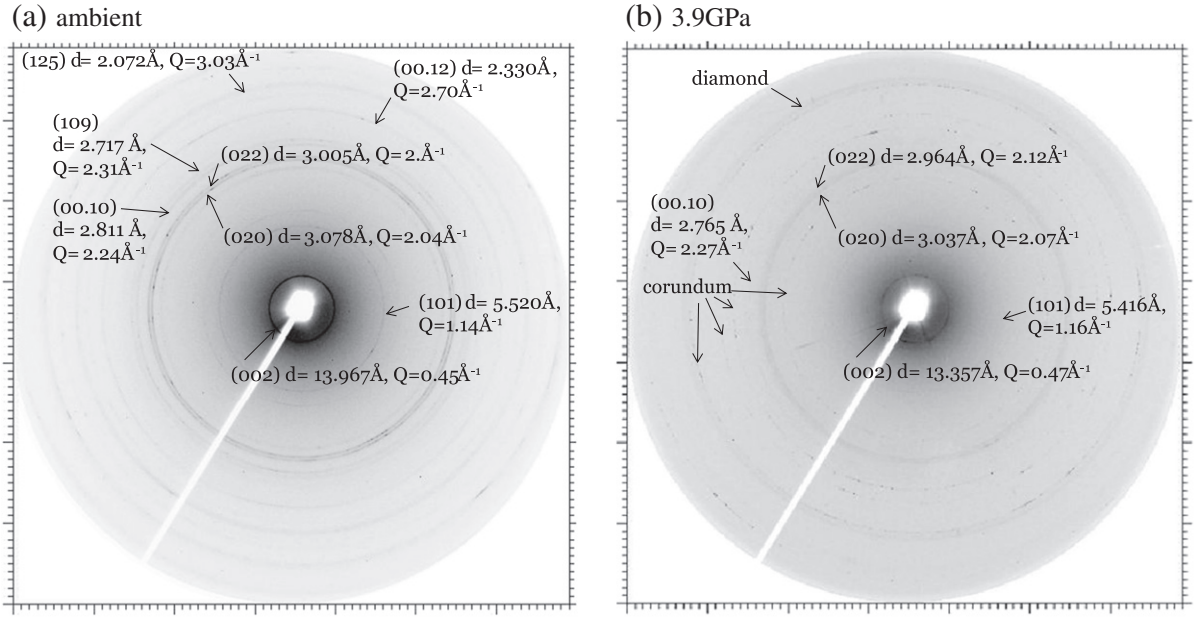

Fig. 3. Synchrotron X-ray diffraction images of 14 Å tobermorite taken under ambient pressure (no DAC used) and at 3.9 GPa (DAC used). The ambient sample did not contain corundum and diamond peaks.

using XFIT may show a large difference from the crystallographic-simulated peak positions.

Thus, JCPDS card #29-0331 was selected as a reference pattern to identify Miller indices, (*hkl*), of the measured diffraction peaks of 14 Å tobermorite because it matched very well with the patterns of current study. However, because the card relies on an orthorhombic crystal system, the calculated lattice parameters and unit cell volume values were converted into monoclinic system for direct comparison with the monoclinic results of Rietveld analysis. Twenty-three diffraction peaks of 14 Å tobermorite were selected for an ambient pattern, but for the high-pressure X-ray diffraction patterns from DAC, only 6 to 8 distinct peaks could be clearly identified because of the small sample size of the DAC apparatus, which made the diffracted intensities very weak. Nonetheless, a reasonable result was obtained. The lattice parameters obtained with the two methods are found to be similar (see Tables 1 and 2).

In the experiment, a third-order Birch–Murnaghan equation of state was fitted to the normalized pressure–volume data to obtain a bulk modulus and the equation is expressed as:

$$P = \frac{3}{2}K_o\left[(V/V_o)^{-\frac{7}{3}} - (V/V_o)^{-\frac{5}{3}}\right]\left[1 + \frac{3}{4}\left(K'_o - 4\right)\left((V/V_o)^{-\frac{2}{3}} - 1\right)\right]$$

where, V is the volume of unit cell, V_o is the initial volume of unit cell at ambient pressure, P is the pressure applied to material, K_o is the bulk modulus at zero pressure, and K'_o is the derivative of bulk modulus at zero pressure [21]. By newly defining the normalized pressure, $F = P/\{1.5[(V/V_o)^{-7/3} - (V/V_o)^{-5/3}]\}$, and the Eulerian strain, $f = 0.5\cdot((V/V_o)^{-2/3} - 1)$, the third order Birch Murnaghan equation of state is reorganized into the linear form: $F(f) = K_o - 1.5K_o(4 - K'_o)f$.

In the plot of F versus f, which were recast from experimental data points, the y-intercept and slope of the weighted least-squares fit gives the bulk modulus K_o and its derivative K'_o at zero pressure (see Fig. 6). To reduce any erroneous effects from all possible errors, a weighted linear least-squares fits with errors [22] was used to modify the standard least-squares regression. Note that the pressure derivative K'_o is quite often assumed to be 4.0, as in the current study based on evidence that the K'_o for many materials approaches 4 [23,24], for low-pressure range studies and high-pressure zeolite studies when the calculated value is considered unrealistic (e.g., too high or too low). Fig. 6 (a) displays the normalized volume-pressure data calculated from the lattice parameters using the Birch–Murnaghan equation. The calculated bulk modulus values are summarized in the figure ($K_o = 47 \pm 3$ GPa from CELREF, $K_o = 47 \pm 4$ GPa from Rietveld method). Fig. 6 (b) shows the f–F curves used to determine the bulk modulus values [25–27].

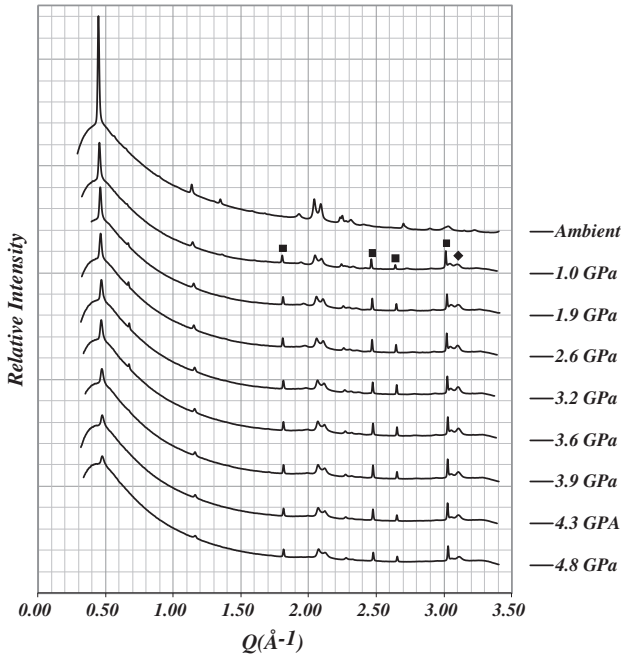

Fig. 4. Integrated powder X-ray diffraction patterns of 14 Å tobermorite by Fit2D as a function of pressure. All the peaks are generated from 14 Å tobermorite except for the peaks indicated with the following labels: ■ = corundum, ♦ = diamond. $Q = 4\pi/\lambda \times \sin(\theta)$; λ = wavelength of incident X-ray in Å, θ = diffracted angle.

4. Discussions

Fig. 7 plots the lattice parameters determined for the current tobermorite sample as a function of pressure, and it also includes the previous study for synthetic C–S–H(I) [= SYN C–S–H(I), Ca/

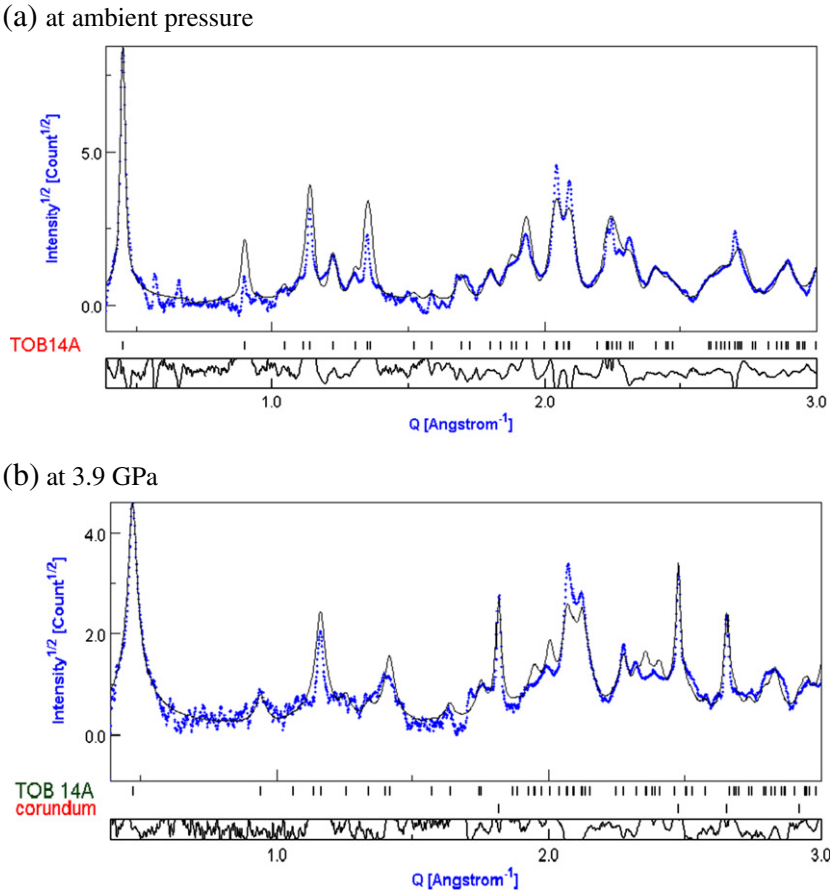

Fig. 5. Refined (solid line) and original experimental (dashed line) profiles from Rietveld analysis of 14 Å tobermorite sample under an ambient pressure and at 3.9 GPa.

Si = 0.97; $\boldsymbol{a}$ = 6.87 Å, $\boldsymbol{b}$ = 7.31 Å, $\boldsymbol{c}$ = 25.34 Å and $\boldsymbol{\gamma}$ = 123.15°, converted into the monoclinic system from the reference data, at ambient condition; K_o of C–S–H(I) = ~38 GPa] by Oh et al. [28]. The new result can be directly compared to results of the C–S–H(I) study because the same experimental techniques were applied. Note that the bulk modulus of 14 Å tobermorite is found to be higher than that of C–S–H(I) by ~24%. Interestingly, while the compression curves of the unit cell parameters $\boldsymbol{a}$ and $\boldsymbol{b}$ for both 14 Å tobermorite and C–S–H(I) are clearly very similar (see Fig. 7), the linear incompressibility of $\boldsymbol{c}$ of 14 Å tobermorite [=~89 GPa/(m/m)] is significantly higher than that of C–S–H(I) [=~61 GPa/(m/m)] by ~45%, suggesting two possible interpretations:

First, although C–S–H(I) is a more disordered form of 14 Å tobermorite [29], they are made up of very similar Ca–O layers that are parallel to the $\boldsymbol{a}$–$\boldsymbol{b}$ plane. Atomic force microscopy measurement [30] supports this assumption by showing surprisingly small changes in these parameters with changes in the Ca/Si ratio. The Fourier transform of the AFM image gave the surface cell parameters ($\boldsymbol{a}$, $\boldsymbol{b}$ and $\boldsymbol{\gamma}$) of C–S–H as a function of Ca/Si. Consequently, although introducing structural disorders into the Ca–O layers (e.g., changes of Ca/Si ratio by omitting bridging Si-tetrahedra in the silicate chains) [8,10] is necessary to reproduce more realistic overall properties of C–S–H, the disorder does not actually change the compression behavior of the $\boldsymbol{a}$–$\boldsymbol{b}$ plane of the unit cell. The Ca–O layer actually controls the compression properties of the $\boldsymbol{a}$–$\boldsymbol{b}$ plane, rather than the silicate chains, or the interlayer molecules and atoms.

Second, the compression behaviors of 14 Å tobermorite and C–S–H(I) are dominated by the characteristics of the interlayer spacing. The interlayer spaces along the lattice parameter $\boldsymbol{c}$ are quite different between these two materials (e.g., different interlayer spacing, interlayer water molecules, degree of disorders in the silicate chains, or additional Ca ions). Note that the bulk modulus values of these two materials are approximately proportional to their linear incompressibility of the lattice parameter $\boldsymbol{c}$. This strongly supports the idea that

Table 1
Pressure–volume data with unit cell parameters for calculated from MAUD software for 14 Å tobermorite as a function of hydrostatic pressure; the calculated unit cell is monoclinic according to reference [13].

P(GPa)	V(Å^3)	a(Å)	b(Å)	c(Å)	γ(°)
Ambient	1153 ± 5	6.7149 ± 0.0005	7.3463 ± 0.0006	27.920 ± 0.001	123.158 ± 0.006
1.0 ± 0.2	1129 ± 20	6.686 ± 0.002	7.329 ± 0.001	27.539 ± 0.004	123.18 ± 0.03
1.9 ± 0.2	1111 ± 7	6.6621 ± 0.0007	7.3100 ± 0.0009	27.274 ± 0.002	123.23 ± 0.01
2.6 ± 0.3	1097 ± 9	6.643 ± 0.001	7.293 ± 0.001	27.060 ± 0.003	123.22 ± 0.01
3.2 ± 0.3	1087 ± 9	6.626 ± 0.001	7.2802 ± 0.0009	26.895 ± 0.003	123.10 ± 0.01
3.6 ± 0.3	1082 ± 6	6.6120 ± 0.0007	7.2884 ± 0.0009	26.799 ± 0.003	123.112 ± 0.009
3.9 ± 0.3	1076 ± 7	6.6108 ± 0.0008	7.2758 ± 0.0007	26.750 ± 0.002	123.22 ± 0.01
4.3 ± 0.4	1063 ± 8	6.5932 ± 0.0009	7.272 ± 0.001	26.471 ± 0.003	123.08 ± 0.01
4.8 ± 0.4	1054 ± 10	6.589 ± 0.001	7.2404 ± 0.0008	26.386 ± 0.003	123.18 ± 0.01

Table 2
Pressure–volume data with unit cell parameters, calculated from CELREF software for 14 Å tobermorite as a function of hydrostatic pressure; the unit cell parameters and volume are calculated using orthorhombic system first according to JCPDS card # 29-0333 and then converted into monoclinic system using the geometrical relationship shown in in-let figure of Fig. 7 in order to directly compare the incompressibility of lattice parameters with the results from Rietveld analysis.

P(GPa)	V(Å^3)	a(Å)	b(Å)	c(Å)
Ambient	577.9 ± 0.4	5.623 ± 0.002	3.677 ± 0.002	27.952 ± 0.006
1.0 ± 0.2	566.5 ± 0.7	5.601 ± 0.004	3.664 ± 0.003	27.61 ± 0.02
1.9 ± 0.2	559 ± 1	5.576 ± 0.004	3.656 ± 0.004	27.40 ± 0.04
2.6 ± 0.3	550.2 ± 0.7	5.555 ± 0.003	3.649 ± 0.002	27.15 ± 0.03
3.2 ± 0.3	545.4 ± 0.9	5.542 ± 0.004	3.643 ± 0.003	27.02 ± 0.04
3.6 ± 0.3	539 ± 1	5.533 ± 0.003	3.640 ± 0.002	26.77 ± 0.07
3.9 ± 0.3	538 ± 1	5.529 ± 0.002	3.637 ± 0.002	26.73 ± 0.06
4.3 ± 0.4	534 ± 2	5.519 ± 0.003	3.634 ± 0.003	26.62 ± 0.07
4.8 ± 0.4	529 ± 2	5.516 ± 0.004	3.629 ± 0.003	26.43 ± 0.09

(a) Lattice parameters and unit cell volumes calculated in orthorhombic cell.

P(GPa)	V(Å^3)	a(Å)	b(Å)	c(Å)	γ(°)
Ambient	1156 ± 1	6.719 ± 0.002	7.354 ± 0.004	27.95 ± 0.01	123.18 ± 0.02
1.0 ± 0.2	1133 ± 1	6.693 ± 0.004	7.328 ± 0.006	27.61 ± 0.02	123.19 ± 0.02
1.0 ± 0.2	1118 ± 2	6.668 ± 0.004	7.312 ± 0.008	27.40 ± 0.04	123.25 ± 0.02
2.6 ± 0.3	1100 ± 1	6.646 ± 0.003	7.298 ± 0.004	27.15 ± 0.03	123.30 ± 0.02
3.2 ± 0.3	1091 ± 2	6.632 ± 0.004	7.286 ± 0.006	27.02 ± 0.04	123.32 ± 0.02
3.6 ± 0.3	1078 ± 2	6.623 ± 0.003	7.280 ± 0.004	26.77 ± 0.07	123.34 ± 0.02
3.9 ± 0.3	1076 ± 2	6.618 ± 0.002	7.274 ± 0.004	26.73 ± 0.06	123.34 ± 0.02
4.3 ± 0.4	1068 ± 4	6.608 ± 0.003	7.268 ± 0.006	26.62 ± 0.07	123.36 ± 0.02
4.8 ± 0.4	1058 ± 4	6.603 ± 0.004	7.258 ± 0.006	26.43 ± 0.09	123.34 ± 0.02

(b) Lattice parameters and unit cell volumes, expressed in monoclinic cell, converted from the values of (a).

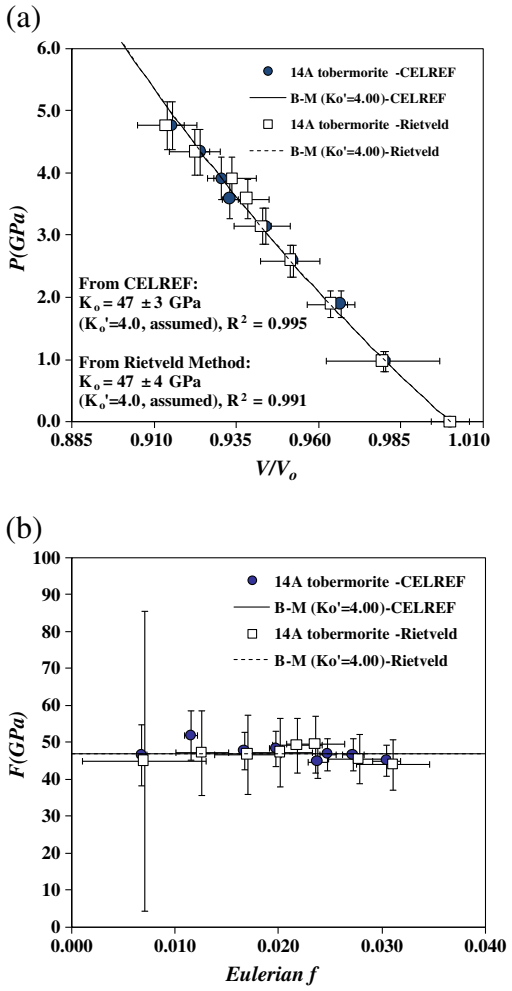

Fig. 6. (a) Pressure vs. normalized volume data of 14 Å tobermorite with its curve-fitted third order Birch–Murnaghan (B–M) equation of state and the calculated bulk modulus values (K_o), and (b) Plot of normalized pressure F versus Eulerian strain f. R^2 = goodness of fit.

further detailed studies for the interlayer space of C–S–H is necessary to understand the properties of C–S–H [32,33].

Molecular dynamics (MD) and ***ab***-initio simulation have played an important role in understanding of C–S–H, and several studies [8–12] have yielded various bulk modulus values for the 14 Å tobermorite (summarized in Table 3). Note the large discrepancies between the MD simulation results, although very similar MD simulation methods were employed. For instance, Al–Ostaz et al's [12] work shows the degree to which the selection of force field and the size of the supercells might influence the simulated result of 14 Å tobermorite in the same MD simulation scheme. Our result for 14 Å tobermorite agrees best with the Manzano et al.'s simulations [8,10] where the bulk modulus of 14 Å tobermorite with infinite length of silicate chains (Ca/Si = 0.83) was 46 GPa and 44.8 GPa; this is very similar to the results presented herein. In addition, they introduced structural defects into the crystal structure of 14 Å tobermorite, thereby limiting the length of silicate chains to the range from dimers to octomers. As the shorter lengths of chains were introduced in [10], the bulk modulus generally decreased in a range of 33.7–47.8 GPa, but mostly the values for 14 Å tobermorite having Ca/Si = ~1.0 are near 35 GPa. These are very close to the experimental result of C–S–H(I) by Oh et al.[28]. On the other hand, our result is higher than the value from the ***ab***-initio calculation by Shahsavari et al. (see Table 3) [11]. However, note that the current 14 Å tobermorite structure by Bonaccorsi et al. does not provide separate positions of H and O atoms of interlayer water molecules and thus the orientations of the water molecules are currently unknown. As seen in Fig. 7, because the atoms and molecules in the interlayer space may largely influence the bulk modulus values of 14 Å tobermorite and C–S–H(I) [32], the orientations of the interlayer water molecules should be also included for more accurate ***ab***-initio simulation. Thus, it is difficult to

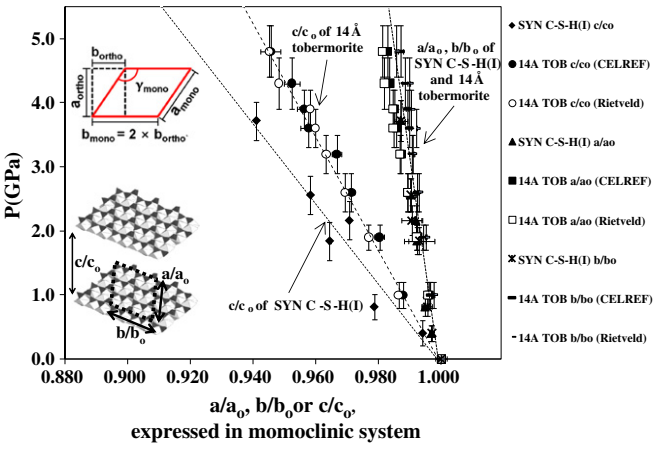

Fig. 7. Incompressibility of normalized lattice parameters ***a***, ***b***, and ***c*** of 14 Å tobermorite of the current study and C–S–H(I) samples from the reference [28]. All lattice parameters are expressed in monoclinic system.

Table 3
Bulk modulus values of 14 Å tobermorite from simulation works in the literature.

Simulation study	Structure Model	Bulk modulus (GPa)	Simulation tool and conditions
Manzano et al. (2007) [8]	Tobermorite 14 Å (Ca/Si = 0.8)	46	Potential minimization (GULP code: general utility lattice program)
Pellenq et al. (2008) [9]	Tobermorite-like 14 Å structure with Ca/Si = 0.83 starting from Hamid's 11 Å tobermorite structure [31]	35.4 (Voigt) 20.7 (Reuss)	Potential minimization (GULP code: general utility lattice program)
Manzano et al. (2009) [10]	Tobermorite 14 Å T∞ (Ca/Si = 0.83)	44.8	Potential minimization (GULP code: general utility lattice program); T = tobermori te; the subscripts OH and Ca refer to the charge used compensation method (see the reference for details); the end number indicates the silicate chain length counted by the number of Si atoms in the chain.
	$T_{Ca}8$ (Ca/Si = 1.0)	47.8	
	$T_{Ca}5$ (Ca/Si = 1.1)	33.9	
	$T_{Ca}2$ (Ca/Si = 1.5)	24	
	$T_{OH}8$ (Ca/Si = 0.94)	36.8	
	$T_{OH}5$ (Ca/Si = 1.0)	33.7	
	$T_{OH}2$ (Ca/Si = 1.25)	26	
Shahsavari et al. (2009) [11]	Tobermorite 14 Å (Ca/Si = 0.83) using Bonaccorsi et al.'s structure [13]	35.91 (Reuss–Voigt–Hill average	First principles study using DFT (density functional theory) and GGA exchange correlation functional, implemented by PWSCF package of quantum espresso
Al-Ostaz et al. (2010) [12]	14 Å tobermorite (Ca/Si = 0.83) using Bonaccorsi et al.'s structure [13]	33.4	1 × single unit cell size with MD tools and force fields = F-U; The same MD method by Manzano et al. (2009). and Pellenq et al.(2008); MD simulation (F = Forcite, D = discover, U = UFF, C = Compass force field), implemented by Materials Studio software
		45.68	1 × single unit cell size with MD tools and force fields = D–C
		49.79	2 × single unit cell size with MD tools and force fields = D-C
		52.89	3 × single unit cell size with MD tools and force fields = D-C

judge each simulation results without any further investigation. Details about the crystal structures at high pressure could be obtained if the Rietveld refinement included atomic positions for which more accurate intensities would be required.

5. Conclusion

The current study experimentally determined the bulk modulus of 14 Å tobermorite, $K_o = 47 \pm 4$ GPa using a Rietveld refinement and $K_o = 47 \pm 3$ GPa from the unit cell parameter refinement using high-pressure synchrotron X-ray diffraction. This study shows that the incompressibilities of the lattice parameters ***a*** and ***b*** are very similar to those of C–S–H(I) determined previously [28], suggesting that the Ca–O layer structures may not be significantly different between 14 Å tobermorite and C–S–H(I). However, the incompressibility of the lattice parameter ***c*** is found to dominantly influence the bulk modulus, implying that the atoms in the interlayer spaces are important in understating the compression behavior of C–S–H.

Previous atomistic simulations for complex C–S–H related materials greatly improved our understanding, but to date were unable to provide a reasonable value for the bulk modulus of 14 Å tobermorite. Presented herein in a method to directly determine the bulk modulus of tobermorite and as such will form an essential constraint for future simulation studies. Urgent future studies include the need to determine the effect of the Ca/Si ratio on the bulk modulus.

Acknowledgments

This publication was based on the work supported in part by Award No. KUS-I1-004021, made by King Abdullah University of Science and Technology (KAUST) and by NIST grant 60NANB10D014. The Advanced Light Source is supported by the Director, Office of Science, Office of Basic Energy Sciences, of the U.S. Department of Energy under Contract No. DE-AC02-05CH11231. The authors thank Dr. Anthony R. Kampf for providing the tobermorite used in this work.

References

[1] J. Birchall, A. Howard, K. Kendall, Flexural strength and porosity of cements, Nature 289 (1981) 388–390.
[2] A.J. Allen, J.J. Thomas, H.M. Jennings, Composition and density of nanoscale calcium–silicate–hydrate in cement, Nat. Mater. 6 (2007) 311–316.
[3] M. Vandamme, F.J. Ulm, Nanogranular origin of concrete creep, PNAS 106 (2009) 10552–10557.
[4] R.J.M. Pellenq, A. Kushima, R. Shahsavari, K.J. Van Vliet, M.J. Buelher, S. Yip, F.J. Ulm, A realistic molecular model of cement hydrates, PNAS 106 (2009) 16102–16107.
[5] I.G. Richardson, The calcium silicate hydrates, Cem. Concr. Res. 38 (2008) 137–158.
[6] H.F.W. Taylor, Proposed structure for calcium silicate hydrate gel, J. Am. Ceram. Soc. 69 (1986) 464–467.
[7] D. Viehland, J.F. Li, L.J. Yuan, Z. Xu, Mesostructure of calcium silicate hydrate (CSH) gels in Portland cement paste: short-range ordering, nanocrystallinity, and local compositional order, J. Am. Ceram. Soc. 79 (1996) 1731–1744.
[8] H. Manzano, J.S. Dolado, A. Guerrero, A. Ayuela, Mechanical properties of crystalline calcium-silicate-hydrates: comparison with cementitious CSH gels, Phys. Status Solidi (a) 204 (2007) 1775–1780.
[9] R.J.M. Pellenq, N. Lequeux, H. Van Damme, Engineering the bonding scheme in CSH: the iono-covalent framework, Cem. Concr. Res. 38 (2008) 159–174.
[10] H. Manzano, J.S. Dolado, A. Ayuela, Elastic properties of the main species present in Portland cement paste, Acta Mater. 57 (2009) 1666–1674.
[11] R. Shahsavari, M.J. Buehler, R.J.M. Pellenq, F.J. Ulm, First-principles study of elastic constants and interlayer interactions of complex hydrated oxides: case study of tobermorite and jennite, J. Am. Ceram. Soc. 92 (2009) 2323–2330.
[12] A. Al-Ostaz, W. Wu, A.H.-D. Cheng, C.R. Song, A molecular dynamics and micro-poromechanics study on the mechanical properties of major constituents of hydrated cement, Composites Part B Eng 41 (2010) 543–549.
[13] E. Bonaccorsi, S. Merlino, A.R. Kampf, The crystal structure of tobermorite 14 Å (plombierite), a C–S–H phase, J. Am. Ceram. Soc. 88 (2005) 505–512.
[14] M. Kunz, A.A. MacDowell, W.A. Caldwell, D. Cambie, R.S. Celestre, E.E. Domning, R.M. Duarte, A.E. Gleason, J.M. Glossinger, N. Kelez, D.W. Plate, T. Yu, J.M. Zaug, H.A. Padmore, R. Jeanloz, A.P. Alivisatos, S.M. Clark, A beamline for high pressure

studies at the advanced light source with a superconducting bending magnet as the source, J. Synchrotron Radiat. 12 (2005) 650–658.
[15] A.P. Hammersley, Fit2d version 12.040, ESRF, Grenoble, France, 2006.
[16] R.W. Cheary, A.A. Coelho, Programs XFIT and FOURYA, deposited in CCP14 Powder Diffraction Library, Engineering and Physical Sciences Research Council, Daresbury Laboratory, Warrington, England, , 1996http://www.ccp14.ac.uk/tutorial/xfit-95/xfit.htm.
[17] J. Laugier, B. Bochu, CELREF, Version 3. Cell parameter refinement program from powder diffraction diagram, Laboratoire des Matériaux et du Génie Physique, Ecole Nationale Supérieure de Physique de Grenoble (INPG), France, 2002.
[18] L. Lutterotti, D. Chateigner, S. Ferrari, J. Ricote, Texture residual stress and structural analysis of thin films using a combined X-ray analysis, Thin Solid Films 450 (2004) 34–41.
[19] R.J. Angel, M. Bujak, J. Zhao, G.D. Gatta, S.D. Jacobsen, Effective hydrostatic limits of pressure media for high-pressure crystallographic studies, J. Appl. Crystallogr. 40 (2007) 26–32.
[20] H.K. Mao, J. Xu, P.M. Bell, Calibration of the ruby pressure gauge to 800 kbar under quasi-hydrostatic conditions, J. Geophys. Res. 91 (1986) 4673–4676.
[21] F. Birch, Elasticity and internal constitution of the earth's interior, J. Geophys. Res. 57 (1952) 227–286.
[22] B.C. Reed, Linear least-squares fits with errors in both coordinates, Am. J. Phys. 57 (1989) 642–646.
[23] E. Knittle, Static compression measurements of equations of state, Mineral Physics and Crystallography: A Handbook of Physical Constants, 1995, pp. 98–142.
[24] G.D. Gatta, Does porous mean soft? On the elastic behaviour and structural evolution of zeolites under pressure, Z. Krist. 223 (2008) 160–170.
[25] F. Birch, Finite strain isotherm and velocities for single-crystal and polycrystalline NaCl at high pressures and 300 K, J. Geophys. Res. 83 (1978) 1257–1268.
[26] C. Meade, R. Jeanloz, Static compression of $Ca(OH)_2$ at room temperature: observations of amorphization and equation of state measurements to 10.7 GPa, Geophys. Res. Lett. 17 (1990) 1157–1160.
[27] R. Jeanloz, Finite-strain equation of state for high-pressure phases, Geophys. Res. Lett. 8 (1981) 1219–1222.
[28] J.E. Oh, S.M. Clark, P.J.M. Monteiro, Does the Al substitution in CSH(I) change its mechanical property? Cem. Concr. Res. 41 (2010) 102–106.
[29] H.F.W. Taylor, Cement Chemistry, 2nd ed. Thomas Telford Services Ltd, London, 1997.
[30] A. Nonat, The structure and stoichiometry of CSH, Cem. Concr. Res. 34 (2004) 1521–1528.
[31] S. Hamid, The crystal structure of the 11 Å natural tobermorite $Ca_{2.25}[Si_3O_{7.5}(OH)_{1.5}]\cdot 1H_2O$, Z. Kristallogr. 154 (1981) 189–198.
[32] A.G. Kalinichev, J. Wang, R.J. Kirkpatrick, Molecular dynamics modeling of the structure, dynamics and energetics of mineral-water interfaces: application to cement materials, Cem. Concr. Res. 37 (2007) 337–347.
[33] S.V. Churakov, Structural position of H_2O molecules and hydrogen bonding in anomalous 11 Å tobermorite, Am. Mineral. 94 (2009) 156–165.